ELSEVIER

Biophysical Chemistry 54 (1995) 43–48

Biophysical Chemistry

Conformational transitions in polyelectrolyte adsorption

O.L. Hörer *, C. Enache

'Stefan S. Nicolau' Institute of Virology, Department of Computer Assisted Research, 285, Sos. Mihai Bravu, R-79650, Bucharest, Romania

Received 16 May 1994; revised 26 September 1994; accepted 3 October 1994

Abstract

The mole fraction X of nucleic acid chromophores, adsorbed on cationic and anionic exchange chromatography paper disks, was calculated [O.L. Hörer and A. Grigorescu, Rev. Roum. Med. Virol., 43 (1992) 33] in terms of the standard Debye screening length D (in the 0.01 to 1.2 M ionic strength range), using data from MLSEA (multiple light scattering enhanced absorption) measurements. In contrast to the cases of mononucleotides or double-stranded and relatively rigid DNA structures, highly polymerized and single-stranded RNA shows sigmoidal-shaped X curves, suggesting that polymer adsorption may be regarded as a conformational transition from a three-dimensional statistical coil to a two-dimensional one.

Keywords: Conformational transition; Polyelectrolyte adsorption; Nucleic acids; Celluloses

1. Introduction

Starting from the standpoint that any thermodynamic phase transition, as represented by the appropriate intensive thermodynamic parameter (e.g. the concentration c_1 of molecular species i in the system, is overruled by molecular long- and short-range forces, it may be presumed that the adsorption of a long polymer chain, such as a nucleic acid, may also be regarded as a conformational transition [1,2]. The biological relevance of conformational transitions occurring in biopolymer adsorption on cell membranes is obvious in gene engineering techniques or in immune processes on cell membranes involving nucleic acids or, respectively, proteins. And the distribution of polymer structural units, estimated as chromophores, between the bulk solution and interface phases can therefore be expressed by a suitable parameter, namely the adsorbed mole fraction.

Any experiment supporting this assumption must take into account the main stages in the polyelectrolyte chain adsorption kinetics, as follows:

(a) A primary adsorption process, which is the result of: (i) the translational diffusion of the whole macromolecule from the bulk phase to the interfacial layer [3]; (ii) reversible conformational transitions [4], determined by the rotational diffusion of the polymer structural units, at first in the field of the long-range forces acting between the electric charged diffusing polyelectrolyte entering into the neighborhood of the also charged interface: at repulsive long-range forces the statistical coil shape changes to a prolate ellipsoid, and to a flat oblate ellipsoid at attractive long-range forces. In the domain of short-

* Corresponding author.

SSDI 0301-4622(94)00121-9

range attractive forces this effect is continued. The relaxation time of this stage is below a second, irrespective of the higher order structure transitions involved [5,6]; (iii) the rapid process of polymer structural units binding to the surface, within the field of all attractive forces, initiating the formation of tails, loops or trains [7,8] in the adsorbed structural units.

(b) A final or secondary adsorption process, of the step by step expansion of the previously formed bonds until true thermodynamic equilibrium is reached. This is affected especially by polymer chain flexibility [7–9], and of a multitude of other conditions.

It was also verified, experimentally [10], and on computer-assisted theoretical models [9], that this secondary adsorption step is the cause of the long polymer adsorption relaxation time so that the end of the primary adsorption process leads to an irreversible adsorption process [11].

Our experimental aim was to restrain the adsorption under room conditions to at least the two rapid stages (ii) and (iii) of the primary adsorption process. Fast drying under air of the previously impregnated paper sheets has been found to be the best procedure to freeze the system in the primary adsorption stage.

2. Materials and methods

Chromatography paper cellulose, a polysaccharide of vegetal cell walls, presents a high stability and reproducibility, being produced in a large variety of ion-exchange standard types, so that it is an adequate model system for cell membranes, having dissociated glycoproteins in the structure of the lipid double layer. Chromatography paper can be regarded as a system with an average distance between the capillary walls of an order of magnitude close to the mean free molecular path [12], so that the running processes are dependent upon the *number* and not upon the *concentration* of the dissolved molecules, and the first step (i) of the primary adsorption stage becomes also quite negligible.

Nucleic acids (RNA, DNA), mononucleotides and uracil chlorhydrate were used as chromophores for the MLSEA (multiple light scattering enhanced absorption) measurements.

2.1. Chromatography paper

Well washed and dried cation exchange Schleicher–Schüll 2043a or Whatman W1, and anion exchange Whatman DE81 and ET81, chromatography paper disks, 6 mm in diameter [13] were used.

2.2. Nucleic acid chromophores

Aqueous solutions containing nucleic acid chromophores in 0.01 to 1.2 M NaCl of about 100 μg/ml were used, corresponding to one of the following substances:

(a) Yeast RNA (Serva),

(b) the corresponding RNA mononucleotides, obtained by alkaline hydrolysis, and neutralization with HCl,

(c) Uracil (Merck), as U. HCl,

(d) Salmon sperm DNA (Mann).

2.3. Samples and references

Each sample paper disk was impregnated with 5 μl of the chromophore solution, and the references with the corresponding chromphore-free solvents, and then allowed to dry for a few minutes in air at room temperature.

2.4. Transmission measurements

The bichromatic absorbances of each paper disk were measured at 260 nm, the characteristic absorption wavelength of nucleic acid chromophores and at 350 nm, a wavelength situated outside the absorption band of the nucleic acid spectrum, using an empirical MLSEA correction formula for the lack of paper homogeneity [13].

A device fitted to a Shimadzu QE50 spectrophotometer was used in all measurements.

The absorbance values were found to be constant over several weeks of storage, demonstrating that the process is actually frozen in the *primary adsorption* state of *metastable equilibrium.*

The experimental points in Figs. 1 and 2 are the averages of corrected absorbance values determined at 260 nm on 5 paper disks. The absorbance values are highly reproducible within a less than 5% relative error, but strongly dependent upon the ionic

strength I of the solutions used for impregnation, and upon the degree of polymerization P of the nucleic acid [14,15].

DNA thermal helix–coil transition data, obtained using paper disk photometry [16], showed that artifacts due to RNA helical loop denaturation, during the experiment, are almost improbable.

The 'optical' mole fraction X, defined as the ratio of the number of chromophores lying in the interfacial layer N_a and the total number N within the paper disk, was calculated on a PC AT 486 computer using theoretical models presented in previous papers [17,18].

Multiple internal reflections produced by total light reflectance amplifies by a factor of G the photon interaction probability (p_c) with the chromophores, inside and in the next neighborhood of the scattering centers, when compared with the corresponding probability (p_i) within the bulk capillary solution, where only external reflection occurs, so that it derives from the well known Judd–Giovanelli [17] equations for the total reflected and normal reflected diffuse light at an interface:

$$G = p_c/p_i = \left[\left(1 - t/(n_c/n_i)^2/(1-t)\right]\right. \quad (1)$$

where t is the normal reflected light fraction, and n_c and n_i are, respectively, the refraction indices of the scattering center and of the capillary solution.

As a corollary of the above statement, the overall molar absorption coefficient K of the added chromophore within the multiple light scattering medium, in terms of the molar absorption coefficient k (in the absence of the MLSEA effect) is:

$$K = 2k[1 + (G-1)X] \quad (2)$$

and the corresponding intrinsic absorption coefficient K_0, in terms of G and k_0 of the scattering centers is:

$$K_0 = 2k_0G \quad (3)$$

The resulting Eq. (4) for the absorbance E of the added chromophores, measured by transmission through a turbid layer of depth d, with a scattering coefficient S is then:

$$E = 0.434 \ln[(aq/b + r)/(a_0q_0/b_0 + r_0)] \quad (4)$$

where $a = a_0 + K/S + 1$, $a_0 = K_0/S + 1$, $b = (a^2 - 1)^{1/2}$, $b_0 = (a_0^2 - 1)^{1/2}$, $q = \sinh Q$, $q_0 = \sinh Q_0$, $r = \cosh Q$, $r_0 = \cosh Q_0$, and $Q = bSd$, respectively,

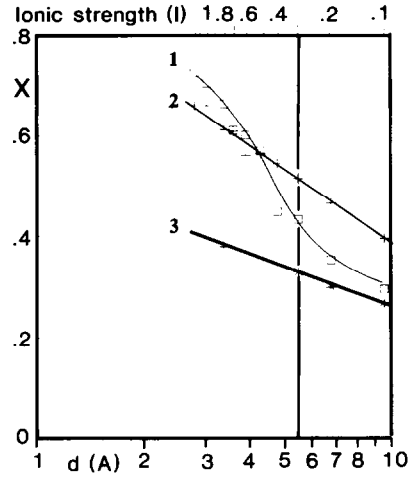

Fig. 1. The mole fraction (X) of nucleotide chromophores adsorbed on Whatman 1 chromatography paper impregnated and allowed to dry with solutions of highly polymerized RNA (curve 1), DNA (curve 2), and RNA mononucleotides (curve 3) in terms of the standard Debye screening length (D), and the ionic strength (I) of the solutions.

$Q_0 = b_0Sd$ are the parameters of the Kubelka–Munk hyperbolic equation [17], the indexes being associated to the intrinsic values of the scattering centers.

It was established [18] that $G = 7.67$, being quite constant for the mean refractive index value $n_c = 1.675$ of the cellulose fibers in the whole experimental range of the salt concentrations used.

The inverse function $X(E)$ was calculated from the absorbance data using computer software described in ref. [18].

3. Results and discussions

In Fig. 1 are shown the X values obtained for RNA (curve 1) DNA (curve 2) and the RNA mononucleotides (curve 3) on cation exchange chromatography papers (Whatman 1 and Schleicher–Schüll 2043a).

Fig. 2 presents the X values corresponding to ARN on the anion exchange chromatography papers ET81 (curve 1) and DE81 (curve 2), and of uracil positively charged ions (curve 3) on cation exchange paper (Whatman 1).

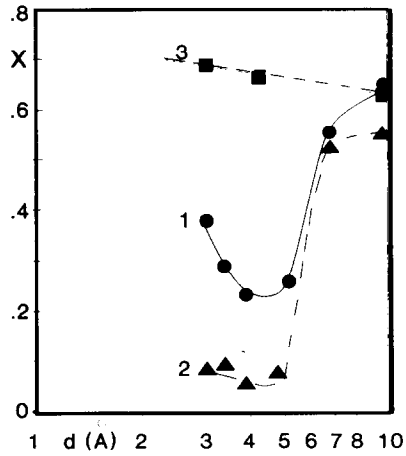

Fig. 2. The mole fraction (X) of RNA nucleotide chromophores adsorbed on ET81 (curve 1), DE81 (curve 2) anion exchange Whatman paper and of uracil hydrochloride on Whatman 1 paper (curve 3) in terms of the standard Debye screening length (D).

The main problem was to choose a suitable parameter, so that the confines of long- and short-range forces could be estimated.

Such a parameter is the standard Debye screening length D expressed in the relation:

$$D = \sqrt{\frac{\epsilon kT \cdot 10^3}{8\pi e^2 NI}}\ 10^{-8}\ \text{cm} \qquad (5)$$

where ϵ represents the dielectric constant of the medium, k the Boltzmann constant, e the electric charge of the electron and N Avogadro's number. The ionic strength I ($\text{mol} \cdot \text{l}^{-1}$) is given, in terms of the c_i molarity and the valence z_i of all i ion species in the solution soaking the paper disk, by $I = (\Sigma c_i z_i^2)^{1/2}/2\ \text{mol} \cdot \text{l}^{-1}$

At 25°C, when $\epsilon = 78.56$ in water, relation 5 becomes:

$$D = \left\{3.03/(I)^{1/2}\right\} \times 10^{-8}\ \text{cm} \qquad (6)$$

In Table 1 are shown a few characteristic D values and the domain of the molecular interaction forces in the 0.01–1.2 M ionic strengths range, the arrows showing the direction of increase:

Above an ionic strength of 0.3 M the interaction corresponds to the attractive Van der Waals, and above 0.6 M the short-range hydrogen bond intermolecular forces are prominent.

Some authors [19–21] have emphasized that below 0.3–0.4 M ionic strength the free electric charge fluctuates along the surface of a polyelectrolyte, being distributed in a diffuse manner, and becomes localized over this I value.

Native or with other ionic groups grafted paper cellulose, shows the same behaviour [22], so that a polyelectrolyte, as the nucleic acid interacts with the light scattering centers of the cellulose fibers at the cellulose–solvent interface, is highly dependent upon the D values for the aqueous phase within the paper capillaries.

The question is, whether the actual salt concentration is that of the impregnating solutions or rather that of the dried paper disks. It was observed by some authors [22,23] that dry paper has a water content of 5 to 10%, in terms of the relative air humidity. The 'dry' paper disks of our experiments had a mean weight of (2.5 ± 0.2) mg, that means less than (250 ± 20) μg water, which corresponds to more than 500 water molecules for 1 nucleic acid chromophore.

Table 1
D values calculated from Eq. (6) in terms of the ionic strength I of aqueous solutions, and the corresponding long- and short-range forces

I (moles/l)	0.01	0.1	0.2	0.3	0.4	0.5	0.6	1.0	1.2
D (Å)	30.3	9.5	6.7	5.47	4.74	4.28	3.86	3.02	2.91

Long-range forces:
(repulsive) ← continuous ion charge ← / ← discrete ion charge ←
(attractive) → continuous ion charge → / → discrete ion charge →

Short range forces:
(attractive) ——→ Van der Waals ——→
(attractive) → H bonds →

In neutral nucleic acid solutions mainly the phosphate groups are dissociated and only a few of the pyrimidine and purine base amino groups, but they are also competing in hydrogen bonds not only within the nucleic acid secondary structure but also with the cellulose OH groups (V. Brumfeld, unpublished infra-red data). There must be, therefore, a net difference between the double-stranded DNA, in which all hydrogen bonds of the bases are taken up by the secondary structure, and the single-stranded RNA, with only a few helical ordered loops. The greatest part of the single-stranded RNA bases and cellulose OH groups are involved in hydrogen bonds with water molecules. But the main difference between the double-stranded DNA and the single-stranded RNA lays in the rigidity [24] of the rod-like shaped DNA structure and, on the other hand, the flexibility of the single RNA chain. Due to the DNA's rigid structure it may be supposed that DNA will interact with cellulose in a way similar to how the small molecules, for instance the mononucleotides, interact with cellulose and most unlike the single-stranded RNA chain.

As the standard errors of all experimental data in Figs. 1 and 2 are smaller than the points represented, they were not shown.

The mole fraction X in Fig. 1 of the chromophores lying within the solution–cellulose interface, are straight lines over the whole I experimental range for DNA (curve 2) [25] and the mononucleotide (curve 3) [26].

In contrast, highly polymerized ribosomal RNA [25] in curve 1 displays a converse sigmoidal-shaped X curve, with a median steep slope in the 5 Å range of D, the region in which repulsive electrostatic long-range forces, acting between both negatively loaded RNA and cellulose, are balanced with the Van der Waals, and at higher I values, also with the hydrogen bond short-range forces.

The observed differences between curve 1, on the one hand, and curves 2 and 3 on the other hand, support the assumption that the flexible single-stranded RNA chain induces a sudden change, and in a cooperative way, of the chromophore distribution when it enters from the capillary bulk phase within the interfacial one.

Strong experimental support for this is to be found in Fig. 2, using positively charged chromatography Whatman papers (ET81 and DE81) with RNA [18,25–27], and uracil hydrochloride on cation exchange paper [26], when only attractive forces are effective throughout.

The difference between the monomer (curve 3) and curves 1 and 2 for RNA in Fig. 2, under the synergetic long- and short-range attractive forces is quite obvious. The flat line of the monomer contrasts with the sigmoidal-shaped cooperative RNA curves.

Another significant comment concerning the above presented data is that, insofar as only the *initial concentration* of the solutions are influencing the adsorption of RNA, the water loss of the paper disks during the fast drying process must be without any measurable consequence on the metastable equilibrium state, reached immediately after the impregnation of the disks.

This supports the following hypothetical statements:

(A) Strong repulsive long-range electrostatic forces between the polyelectrolyte chain and the surface allow the polymer form only short tails, the major part of the prolate coil remaining far from the surface, even during the drying process. When, at the initial higher ionic strength, the long-range repulsive forces reach the same magnitude with the short-range attractive ones, the discrete surface charge distribution [19] permits the loops, and, only on the larger, uncharged interfacial regions, trains to be formed in an irreversible way.

At increasing attractive forces, the shape of the isometric statistical coil changes to a thinner and thinner oblate form, so that, by extrapolating $X = 1$, the shape of the polymer must change to a two-dimensional coil.

The sharp X-value change in a close standard Debye screening length D range indicates a cooperative conformational transition.

(B) At high and opposite electric charges of the surface and polyelectrolyte, at low ionic strength, the chromophores will spread out ab initio in the vicinity of the surface and the polymer will be able to form trains on the adsorbing surface. Their length and number will decrease at increasing ionic strengths, so that X will show a sharp decrease at ionic strength values above 0.3 M, as Van der Waals forces act on the polymer chain, stretching it out.

(C) An explanation for the negative slope of the

RNA X curves in both figures, corresponding to higher than 0.6 M ionic strength, is correlated with the effect of the high salt concentration on the increase of the hydrogen bond formation probability between the polymer and the adsorbent, the solvated salt ions competing in the water hydrogen bond equilibria.

If such cooperative conformational transitions, as suggested by the data presented and discussed above, are involved also in other biopolymer adsorption processes in living systems, which are taking place under similar conditions, then the experimental model used illustrates the importance of the long-range forces on the true interacting conformation, resulted during the diffusion of the polymer chain in the neighborhood of the interface.

In most papers published on similar subjects the statistical three-dimensional coil conformation of the biopolymer chains in the bulk solution is used for modeling the adsorption process. No relevant conformational transitions of polyelectrolytes in the field of long-range forces acting between the polymer chain and the biologic surfaces have yet been taken into account.

4. Conclusion

The presupposition of the cooperative character of linear polyelectrolyte adsorption on ionized surfaces, in terms of the ionic strength, is supported by MLSEA measurements on cation and anion exchange chromatography paper disks, impregnated with highly polymerized RNA solutions and allowed to dry.

The cooperativity of this adsorption process is correlated positively with the degree of polymerization, and negatively with the rigidity of the polymer chain.

A conformational transition from a three-dimensional to a two-dimensional statistical coil can be claimed for the adsorption of nucleic acid chains, and of other polyelectrolytes.

Acknowledgements

This work was supported by grant ERB CIPECT 926095.

References

[1] R.R. Stromberg, D.J. Tutas and E. Passaglia, J. Phys. Chem., 69 (1965) 3955.
[2] A. Bellemans and J. Orban, J. Chem. Phys., 75 (1981) 2454.
[3] Z. Morita, T. Tanake and H. Motomura, J. Appl. Polym. Sci., 30 (1985) 3697.
[4] M.K. Graufeldt, Bo Jönsson and C.E. Woodward, J. Phys. Chem., 95 (1991) 4819.
[5] R.G. Pain, Nature, 358 (1992) 278.
[6] E.S. Radford, C.M.A. Dobson and P.A. Evans, Nature, 358 (1992) 302.
[7] A. Silberberg, J. Phys. Chem., 66 (1962) 1872, 1884.
[8] F.Th. Hesselink, J. Chem. Phys., 52 (1970) 2567.
[9] A. Silberberg in L.H. Lee (Editor), Adhesion and Adsorption of Polymers, Plenum Press, New York, 1980, pp. 591–600.
[10] Y. Ishimaru and T. Lindström, J. Appl. Polym. Sci., 29 (1984) 1675.
[11] X. Jin, N.-H. Linda, G. Tarjus and J. Talbot, J. Phys. Chem., 97 (1993) 4526.
[12] J. Pochly, J. Chem. Phys., 52 (1970) 2567.
[13] O.L. Hörer and M. Popescu, Anal. Chim. Acta, 35 (1966) 6.
[14] O.L. Hörer, Kolloid Z.Z. Polym., 209 (1966) 180.
[15] O.L. Hörer, Kolloid Z.Z. Polym., 236 (1970) 175.
[16] O.L. Hörer, Rev. Roum. Med. Virol., 34 (1983) 223.
[17] O.L. Hörer, Rev. Roum. Med. Virol., 37 (1986) 181.
[18] O.L. Hörer and Adriana Grigorescu, Rev. Roum. Med. Virol., 43 (1992) 33.
[19] G.S. Manning, Quart. Rev. Biophys., 11 (1978) 181.
[20] G.W. Ramanathan and C.P. Woodbury Jr., J. Chem. Phys., 77 (1982) 4133.
[21] Bo Svensson, Bo Jönsson and C.E. Woodward, J. Chem. Phys., 94 (1990) 2105.
[22] S. Sapicha, M. Inoue and P. Lepoutre, J. Appl. Polym. Sci., 30 (1985) 1257.
[23] F. Onabe, J. Appl. Polym. Sci., 22 (1978) 3495; 23 (1979) 2909.
[24] E.A. DiMarzio, J. Chem. Phys., 66 (1977) 1160.
[25] O.L. Hörer and C. Enache, Rev. Roum. Med. Virol., 34 (1983) 177.
[26] O.L. Hörer, Rev. Roum. Med. Virol., 35 (1984) 139.
[27] O.L. Hörer and C. Enache, Rev. Roum. Med. Virol., 35 (1984) 31.